A Novel Antenna Isolation Method for Mobile Phone Antennas

Corbett Rowell
Electrical & Electronic Engineering Department
University of Hong Kong
Applied Science and Technology Research Institute (ASTRI)
Science Park, Hong Kong
Email: corbett@astri.org

Edmund Y. Lam
Electrical & Electronic Engineering Department
University of Hong Kong
Pokfulam, Hong Kong
Email: elam@eee.hku.hk

***Abstract*—The behavior of a two element antenna system within a mobile phone where one antenna has a particular slot configuration, designed to reduce the mutual coupling of the two antennas at a particular frequency corresponding to the length of the slot and the ground and feed placement, is analyzed and measured. This particular set of antenna geometries can create a large group delay at certain frequencies, significantly increasing the isolation between the two antennas. A large group delay can reduce the mutual coupling between two antenna by over 25 dB compared to a non-optimized system. By reducing the mutual coupling, the radiation efficiency increases by 20-30%. This paper analyzes the two antenna system within a mobile phone where the first antenna is GSM + 3G and the second antenna is 4G where the 4G frequency band directly overlaps with the 3G frequency band.**

I. Introduction

This paper analyzes an antenna modification of a long slot between the ground and feed locations in one of the antennas in a two antenna element system designed for a mobile phone with GSM, 3G, and 4G standards similar to the antenna isolation method discussed by the author in the IEEE APS 2006 conference [1]. The antenna geometry presented in that conference use S-Parameters to analyze two slots that provide isolation, but did not propose a generalized solution or a physical understanding of the isolation mechanism. This paper uses a single slot and demonstrates that the placement of the ground and the feed is critical to the antenna isolation. Furthermore, this paper uses group delay analysis to illustrate the isolation mechanism of the antenna modification.

A. Methodology & Background

1) Measurements: For the passive antenna measurements, the RF cable is routed through the prototype and exits the prototype in an area that causes the least disturbance to the EM field distribution of the antenna (typically in the center of the PCB since the current distribution will often be high at both ends of the PCB). A Rohde & Schwarz ZVB Vector Network Analyzer was used for the S-parameter measurements and a Satimo Starlab system was used to measure the 3D radiation patterns, antenna efficiency, and antenna gain [2].

2) Simulations: CST Microwave Studio [3] was used to calculate the electric and magnetic field distributions for the antennas in order to illustrate the physical behavior of the two antenna system; assuming Perfect Electric Conductor (PEC) for all metals and ABS-Plastic of $\epsilon = 3.0$ for the antenna carrier.

3) Group Delay Calculations: Group delay is normally used for filter design to characterize the distortion of a broadband signal inside the filter and filter designers typically design the filter such that the group delay is the same for all frequencies [4]. Group delay is also an important parameter for the design of UWB and GPS antennas since some UWB/GPS systems are very sensitive to signal timing and phase distortions [5], [6]. In addition to characterizing the signal distortion, group delay can be used to analyze the mutual coupling between antennas, or S21. Recently, there have been a couple papers analyzing new antenna structures with very sharp S21 response at particular frequencies with S21 lower than -30dB [7], [8]. In all of these antenna geometries, the group delay at that frequency is much greater than for the rest of the signal bandwidth.

The group delay of the phase response is the negative derivative of the phase response as a function of frequency:

$$S'_{21} = -\frac{\partial S_{21}\angle}{\partial f}$$

where $S_{21}\angle$ is the unwrapped phase response. By converting both frequency and the phase angle to degrees, the group delay can be quickly calculated in units of GHz and nanoseconds.

B. Antenna Description

This paper considers three sets of antennas. The first two sets, referred to as "Basic Antenna Geometry", compare the effect of the feed and ground placement, while keeping all other parameters the same. The first Basic Antenna geometry, BA^{right}, situates the feed on the right of the slot; whereas the second Basic Antenna geometry, BA^{left} reverses the feed and ground location such that the feed is on the left side of the slot. The third set, referred to as "Optimized Antenna Geometry" or OA, optimizes the antenna geometry in order to achieve best S21 and 3D radiation efficiency.

The Basic Antenna is a two antenna system in Figure 1 that has one PIFA antenna for quad-band GSM (BA_1) and a second PIFA antenna for 3G/4G operation (BA_2). The first antenna, BA_1 has a slot cut into the antenna between the feed and the ground where the placement of the feed and ground connections is critical for the creation of the S_{21} "null" seen in Figure 4 since the placement determines the current vectors on the antenna (clockwise vs counter-clockwise). The slot has a total length of $59.5mm$ from the base of the feed/ground connection to the PCB at the end of the slot, corresponding to an operating frequency of $f = 2.54\,GHz$. The dielectric loading of the antenna carrier in addition to the inductive loading effects of the bends in the slot arrangement further decrease the slot's resonant frequency to $f^{slot} = 1.92 - 2.07\,GHz$ for the three antenna geometries. At this frequency, the slot has similar behavior to a $\lambda/2$ slot antenna (magnetic field antenna). The second antenna, BA_2 is a PIFA antenna with dimensions $\{L_1,\, L_2,\, H\} = \{21, 8.5, 10\}\,mm$, and a resonant frequency of $f_{BA2}^{PIFA} = 2.0\,GHz$, demonstrating similar performance characteristics as a $\lambda/4$ monopole (electric field antenna). The first antenna, BA^{right} has an additional PIFA-mode resonance at $f_{BA1}^{PIFA} = 1.00\,GHz$ and BA^{left}, $f_{BA2}^{PIFA} = 1.05\,GHz$.

The Optimized Antenna geometry in Figure 2 is similar to the Basic Antenna, with a no frequency shift for first antenna in the lower frequency band of $f_{OA1}^{PIFA} = 1\,GHz$, a slot frequency of $f^{slot} = 2.07\,GHz$, and a frequency shift for the higher band in the second antenna of $f_{OA2}^{PIFA} = 1.92\,GHz$.

C. Measurement & Simulation Results

1) S-Parameters Measurements: Prototypes were constructed using FR4 PCB, Copper Tape, and a plastic ABS carrier. The S-parameters were measured after adjusting for the correct phase delay due to the measurement cables and the results are shown in Figures 3 and 4. The GSM antenna is port 1 and the 3G/4G antenna is port 2. The optimized antenna, OA, has a sharper S11 resonance in the upper frequency band for the GSM antenna; but worse S11 for the 3G/4G antenna. The S22 resonance for the Basic Antenna geometry is slightly different for the BA^{left} and BA^{right} due to the difference in coupling between the 3G/4G antenna and the GSM antenna. The biggest difference in performance can be seen from the S21 measurements. Although the geometry of both Basic Antennas is the same and the S11/S22 parameters are not significantly different, the reversal of the feed and ground has a significant effect on the S21, leading to a "null" at 1.9 GHz with an S21 difference of 8 dB. Further optimization of the slot in the OA geometry not only increases the S11 performance at the upper frequency band, but also gives a S21 difference of over 25 dB at 2.07 GHz.

2) Group Delay Calculations: The group delay calculation illustrates the differences between the S21 coupling characteristics more clearly than the S-parameter matrix. A typical S21 curve does not have a sharp difference in phase, but a null in the S21 parameter has a significant change in phase over a short time, leading to a higher group delay at that set of frequencies. Figure 5 plots the group delay for all three antenna geometries. The optimized antenna geometry has the the highest group delay, corresponding to the lowest S21 of -42 dB at $2.07\,GHz$ and the best 3D radiation efficiency of 72%.

3) Electromagnetic Field Simulations: As illustrated in Figures 6 & 7, the slot excites the magnetic field in the first antenna, BA_1; whereas the electric field is excited in the second antenna, BA_2. The current vector is reversed in the middle of the slot, indicating a $\lambda/2$ resonance. By reversing the feed and ground locations in the Basic Antenna geometry, the phase of the current is also reversed, as seen in Figures 7 & 8. For the antenna with the S21 anti-resonance (BA^{right}), the phase of the current in the slot when the first antenna is excited, J_{BA1}^{slot}, is 180 degrees out of phase with the coupled current in the slot when the second antenna is excited, J_{BA2}^{slot}. When the feed and ground connections are reversed (BA^{left}), then the two currents are in phase: $J_{BA1}^{slot}(\phi) = J_{BA2}^{slot}(\phi)$.

The reversal of the feed and ground locations do not change the general far-field pattern, but does have a significant effect on the radiation efficiency, as demonstrated in the measurement results.

4) Radiation Efficiency Measurements: Both the OA and BA^{right} with the special slot and feed/ground arrangement had a 20-30% improvement in 3D radiation efficiency in the GSM antenna when compared to BA^{left} , whereas the 3G radiation efficiency is not significantly affected, as seen in Figure 9.

II. Conclusions

In this paper, a slot with a specific feed and ground placement is proposed as a method to reduce isolation at a particular frequency. The slot creates an additional resonance within the PIFA and can be easily adjusted to match the same resonance as the adjacent antenna. By placing the feed to the right of the slot and the ground on the opposite side, there is a phase delay introduced into the system. This phase delay, characterized by a high group delay, reduces the S21 at that frequency by over 25 dB, and increases the 3D radiation efficiency by 20-30%.

Acknowledgment

The authors would like to thank and acknowledge the contributions made by the ASTRI Antenna team [9].

References

[1] C. Rowell, A. Mak, and C. L. Mak, "Isolation between multiband antennas," *IEEE APS/URSI/AMEREM Int. Symp.*, Albuquerque, NM, pp. 551–551, July 2006.

[2] Satimo [Online]. Available: http://www.satimo.fr/eng/index.php).

[3] CST Microwave Studio 2006B by Computer Simulation Technology [Online]. Available: http://www.cst.com.

[4] L. D. Paarmann, "Design and analysis of analog filters: a signal processing perspective", *Kluwer Academic Publishers*, pp. 225-230, 2001.

[5] D. H. Kwon, "Effect of antenna gain and group delay variations on pulse-preserving capabilities of ultrawideband antennas", *IEEE Trans. Antennas Propag.*, Vol. 54, No. 8, pp. 2208-2215, August 2006.

[6] W. Gong, D. R. Jackson, and J. T. Williams, "Phase and group delays for circularly-polarized microstrip antennas", *IEEE APS/URSI/AMEREM Int. Symp.*, Albuquerque, NM, pp. 1537–1540, July 2006.

[7] C.-Y. Chiu, C.-H. Cheng, R. D. Murch, and C. R. Rowell, "Reduction of mutual coupling between closely-packed antenna elements," *IEEE Trans. Antennas Propag*., vol. 55, no. 6, pp. 1732–1738, Jun. 2007.
[8] A. C. K. Mak, C. R. Rowell, and R. D. Murch, "Isolation enhancement between two closely packed antennas", *IEEE Trans. Antennas Propag*., vol. 56, no. 11, pp. 3411-3419, Nov. 2008.
[9] Angus Mak, Irene Cheung, Wilfredo Daluz, Alan Mak, Ho Kin Lun, and Tim Chan, *ASTRI Antenna Group*

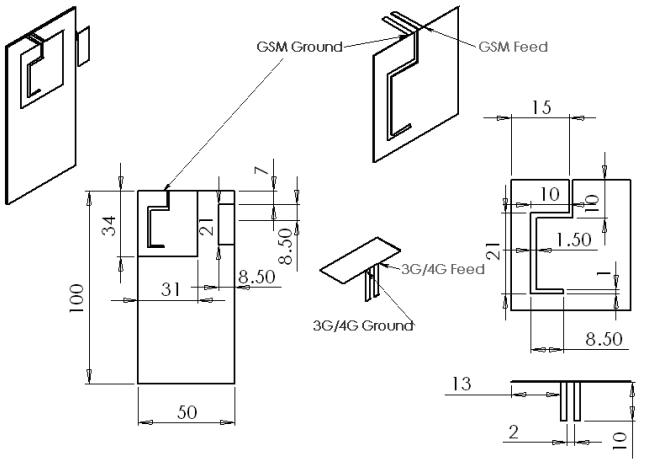

Figure 1. Geometry of Basic Antenna with slot between the ground and feed for both BA^{right} and BA^{left}. For BA^{left}, the ground and feed locations are reversed for the the GSM antenna (not the 3G/4G antenna).

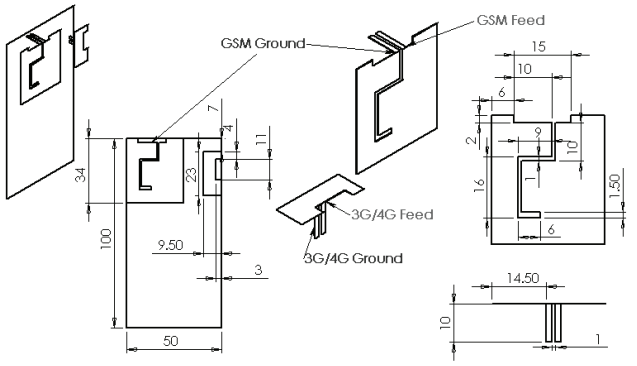

Figure 2. Geometry of the Optimized Antenna, OA with optimization of the S21 null. Most of the geometry is similar to the Basic Antenna, but with inset feeds for both GSM & 3G/4G antennas.

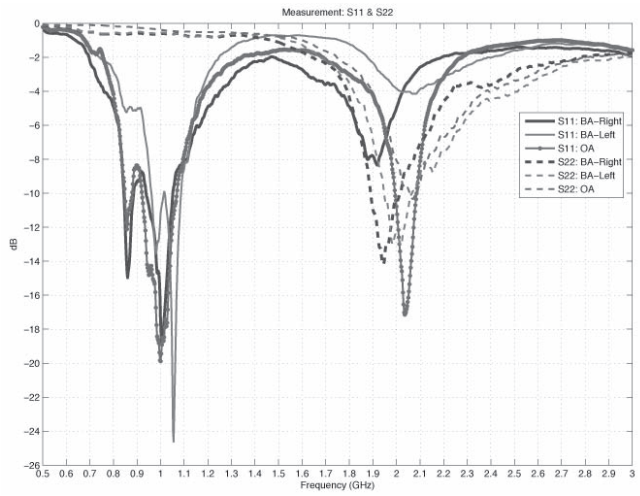

Figure 3. Measurement of S11 & S22 for the three antenna geometries.

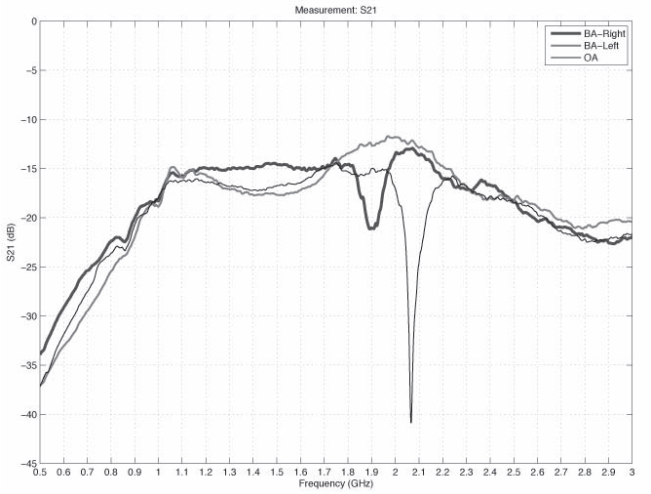

Figure 4. Measurement of S21 for the three antenna geometries.

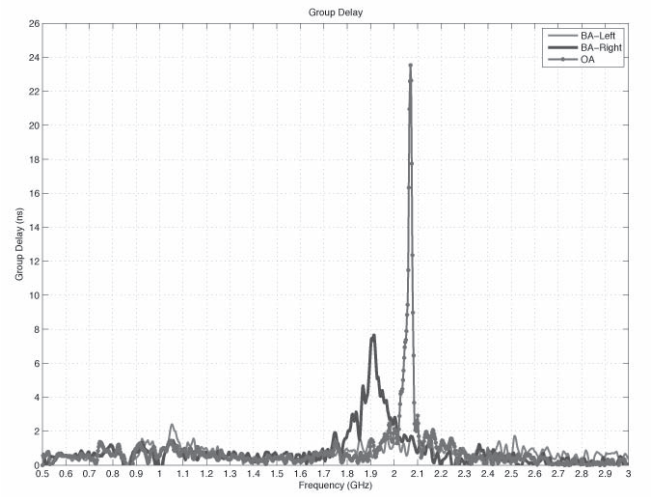

Figure 5. Group Delay calculations from the measurement results for the three antenna geometries.

Figure 6. Electric & Magnetic Field Distributions for the BA^{right} geometry at $f = 1.99\,GHz$. The field distributions are the same for both the BA^{right} and the BA^{left} geometries. On the left is the magnetic field distribution for the GSM antenna and on the right is the electric field distribution for the 3G/4G antenna. (Dark grey is zero field and lighter greys represent stronger field strength).

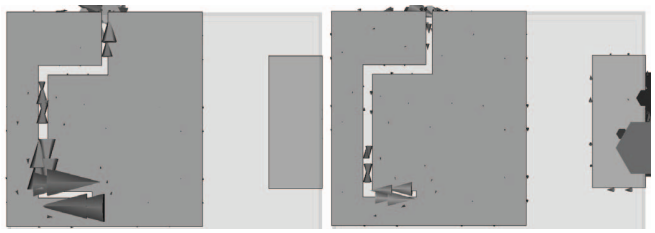

Figure 7. Current Distributions on BA^{right} GSM & 3G antennas at $f = 1.99\,GHz$. On the left is the GSM antenna (port 1) excited and on the right is the 3G/4G antenna excited (port 2).

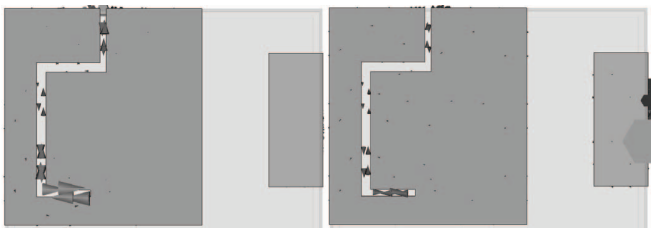

Figure 8. Current Distributions on BA^{left} GSM & 3G antennas at $f = 2.07\,GHz$. On the left is the GSM antenna (port 1) excited and on the right is the 3G/4G antenna excited (port 2).

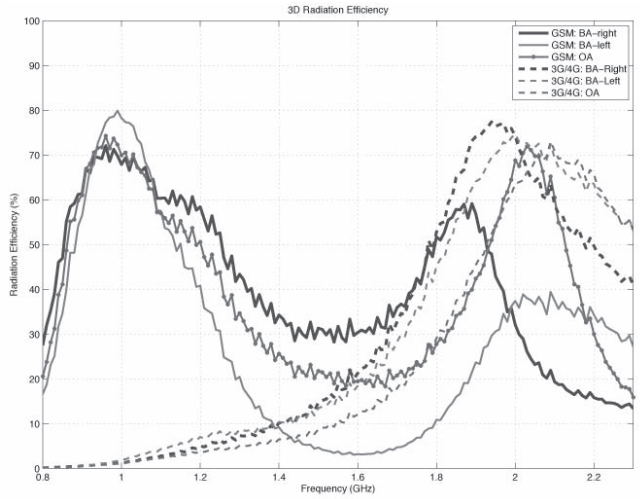

Figure 9. Radiation Efficiency for the GSM antenna in BA^{right}, BA^{left}, OA geometries.